Materials Characterization 130 (2017) 50–55

Contents lists available at ScienceDirect

Materials Characterization

journal homepage: www.elsevier.com/locate/matchar

Thickness determination of anodic titanium oxide films by electron probe microanalysis

Kyung Won Kang[a], Silvina Limandri[b], Gustavo Castellano[b], Sergio Suárez[c], Jorge Trincavelli[b,*]

[a] Laboratorio de Investigaciones de Metalurgia Física "Ing. Gregorio Cusminsky" (LIMF), Facultad de Ingeniería, Universidad Nacional de La Plata, Calle 1 y 47, La Plata, Buenos Aires 1900, Argentina

[b] Instituto de Física Enrique Gaviola (IFEG), CONICET, Facultad de Matemática, Astronomía, Física y Computación, Universidad Nacional de Córdoba, Medina Allende s/n, Ciudad Universitaria, Córdoba 5000, Argentina

[c] Centro Atómico Bariloche (CAB-CNEA) and CONICET, Av. E. Bustillo 9500, San Carlos de Bariloche, Río Negro 8400, Argentina

ARTICLE INFO

Keywords:
Titanium implants
Anodic oxidation
EPMA
RBS

ABSTRACT

Thin film thickness can be readily associated to the X-ray intensities emitted under electron bombardment. The aim of this work is to develop a method for measuring titanium oxide thicknesses in biomaterials from the X-ray spectra induced in a scanning electron microscope. The oxide layers studied were generated with different anodizing voltages applied in phosphoric and boric acid solution (H_3PO_4/H_3BO_3). The oxygen Kα intensity was registered for each sample and related to the corresponding thickness. In order to account for local material alterations, a recalibration is shown to be necessary; Rutherford backscattering spectroscopy was used at this stage. The method is useful for TiO_2 thicknesses in the range of interest for dental and orthopedic implants (10–100 nm), and it could be extended to greater thicknesses by adequately selecting the electron beam energy.

1. Introduction

Titanium is a biomaterial widely used in dental and orthopedic implants, because it combines good corrosion resistance with high biocompatibility properties [1–3]. This material typically bears a spontaneous thin oxide layer from 1.5 to 10 nm thick [4], which may be regarded as bioinert, since it is quite stable and induces no adverse reactions in human body fluids and tissues [1,2]. For this last reason, titanium osteoinductive capacity is poor or null; nevertheless, it is often considered as an osteoconductive biomaterial, since it provides scaffolds for bone tissue formation, though only physical adsorption is allowed and the osseointegration of these implants depends on the materials surface characteristics [5]. The biomaterial surface plays an essential role in the biological environment response to these implants; depending on the specific situation, different surface treatments can be consequently applied in order to speed up the bone development and to improve the implant-bone integration.

Anodization is a treatment which produces different types of metal oxide films. Several acids and bases are generally used in this process – H_2SO_4, H_3PO_4, HNO_3, CH_3COOH, $Ca(OH)_2$, Na(OH), etc. The chemical structure and properties of the passive layer depend on the anodizing parameters such as anode potential, electrolyte composition, temperature and current [1,6,7]. The main advantages of titanium anodizing are the growth of a layer with high adhesion to substrate [1], and the increase in the passive oxide thickness, which influences the interaction with the biological environment [6,8] and improves corrosion resistance [2]. Particularly, anodization in phosphoric acid offers some advantages as compared to other electrolytes, because it allows to produce compact tubular or porous oxide layers, and considerably improves biocompatibility properties, due to the incorporation of phosphate ions into the oxide layer [9].

A proper knowledge of the Ti oxide thickness after anodization is important, because this parameter influences the implant performance. Several techniques have been applied to face this issue for different anodization conditions, such as: light reflectance spectrophotometry [10], Rutherford backscattering spectroscopy [11], Auger spectroscopy [12] and atomic force microscopy [8], comprising different anodizing voltage ranges (AV) 5–80 V, 20–84 V, 20–130 V and 50–250 V, respectively, and thicknesses d greater than 30 nm. Regarding transmission electron microscopy, it must be noted that this technique, in principle, allows for a direct inspection of the sample; nevertheless, it would require the preparation of well defined cross section samples, difficult to achieve. In addition, transmission electron microscopy involves a very small sample region, not representative of large areas, more suitable for the kind of samples studied here.

Recently, a method for thickness determination based on electron

* Corresponding author.
E-mail address: trincavelli@famaf.unc.edu.ar (J. Trincavelli).

http://dx.doi.org/10.1016/j.matchar.2017.05.027
Received 26 October 2016; Received in revised form 17 May 2017; Accepted 17 May 2017
Available online 18 May 2017
1044-5803/

irradiation was developed. This approach relies on the dependence of the characteristic oxygen Kα X-ray emission intensity on the layer thickness, and uses ellipsometry as a reference calibration technique [13]. With this method, titanium oxide films potentiodynamically grown on top of titanium substrates using a 0.01 M $HClO_4$ solution and anodizing voltages between 1 and 10 V were characterized, obtaining reliable results. In the development of the mentioned approach, the oxide growth rate with the anodizing voltage was found to be much lower than expected. From this result and studying the specimen current evolution during spectrum acquisition, the authors concluded that the sample is modified by the incident electron beam, which probably causes the migration of O atoms from the incidence beam spot. For this reason, it is not possible to obtain a straightforward method for the determination of thicknesses by EPMA. To solve this problem, the authors found a relationship between the experimental O-Kα peak intensity and the anodizing voltage, which was associated with the oxide thickness by using ellipsometry as a reference technique. This technique permits to obtain a relationship between the oxide thickness and the anodizing voltage, so that in a further step, the O-Kα peak intensity can be used to determine the thickness of oxide layers electrochemically formed with different anodizing voltages. In the mentioned paper, the calibration was performed for TiO_2 films grown by anodization in a 0.01 M $HClO_4$ solution, with voltages between 1 and 10 V. In the present work, the method developed by Filippin et al. [13] is extended to anodizing voltages in the 5–90 V range, using RBS as reference technique.

Titanium oxide thicknesses, were produced by anodization in a 1% H_3BO_3/5% H_3PO_4 (%p/p) solution with voltages between 5 and 90 V. Recalibration through Rutherford Backscattering Spectroscopy (RBS) is applied, allowing for the extension of the method to thicknesses corresponding to a wider voltage range, more adequate for the dental and orthopedic implant field of interest. It is worth mentioning that once the recalibration is accomplished, RBS is not needed any more if other samples of the same type (TiO_2 film on Ti) are to be characterized; instead, only electron probe microanalysis (EPMA) is required, a more economic and accessible technique.

2. Materials and Methods

2.1. Sample Preparation

Commercially pure ASTM grade 4 titanium (0.0039% N, 0.0112% C, 0.11% Fe, 0.24% O, 0.00% H, Ti BAL) was used for the present study. Anodization treatments were applied to two sets of machined cylinders: one with 6-mm diameter and 3-mm height (type 1), and the other one with 10-mm diameter and 4-mm height (type 2).

The first step in the sample preparation consisted of descaling during 1 min in a 1% HF/5% H_2SO_4 (%p/p) solution. Then, the samples were anodized in a 1% H_3BO_3/5% H_3PO_4 (%p/p) solution at room temperature, adjusting the potential at different values between 5 and 90 V. The procedure was carried out by performing a galvanostatic anodizing for each voltage, i.e., the current was kept constant (2 A for all the voltages) during the time needed to reach each pre-established potential. Finally, the samples were washed with distilled water two times, dried and individually packaged in polyethylene films.

The voltages applied for anodizing were 5, 10, 15, 20, 25, 50, 70 and 90 V for type 1 samples and 30 V for the type 2 sample. The anodizing treatments were performed using a source Sorensen DLM 600-5E 3 kW, 0–600 V, 0–5 A.

2.2. RBS and EPMA Measurements

The RBS spectra were generated using 2.00, 3.04 and 3.05 MeV alpha particles. The incident beam impinged the samples perpendicularly and the backscattered α particles were detected with a surface barrier detector set at 165° with respect to the incident beam direction. Measurements were carried out using a 1.7 MV Tandem accelerator.

Regarding the X-ray spectra induced by electrons, they were obtained with a JEOL JXA 8230 microprobe, taking advantage of the wavelength dispersive spectrometer (WDS) attached to this equipment. The high resolution of the WDS used allows to resolve the strong overlapping between the oxygen Kα line and the titanium L lines. Samples were irradiated using a 4 keV electron beam with a current between 79.7 and 80.4 nA. The X-ray spectrum was acquired using an LDE1 crystal with a front mylar window, photon energies ranging from 467 to 583 eV, with a 0.002 Å step between channels. For all measurements the dwell time was 1.3 s per channel.

3. Results and Discussion

In an EPMA experiment, the incident electrons undergo a large number of interactions with the target atoms and can be completely stopped within the sample if it is thick enough (around 150 nm in TiO_2 for 4 keV electrons, according to an estimation performed using the Kanaya-Okayama formula). In the case of a sample composed by a TiO_2 nanometric layer grown on a titanium substrate, the larger the thickness of the oxide layer, the more intense the O-Kα peak detected. This behavior, however, is no longer exhibited when the oxide layer thickness is similar to or higher than the electron range. For this limiting case, the electrons are completely stopped within the oxide, and a thicker oxide layer would not contribute with additional O-Kα photons. The relationship between the O-Kα peak intensity and the film thickness was investigated by means of Monte Carlo simulations using the PENELOPE software package, in order to find a convenient value for the electron incident energy [14]. It was found that for the thickness range involved, 4 keV electrons allows for an application of the method proposed with an appropriate sensitivity.

3.1. RBS

Thin film characterization is one of the main applications of Rutherford backscattering spectroscopy. Multilayered materials, surface and subsequent interfaces can be studied by means of the backscattered particle signal. Two independent magnitudes can be obtained from the RBS spectrum: the energy width ΔE between the signal edges corresponding to adjacent interfaces, and the total number of counts included in the spectral interval between both edges. From these values, the number of atoms per unit area contained in the corresponding layer can be obtained. When the film is composed by more than one element forming a homogeneous mixture, the contribution of each element to the backscattered spectrum can be deconvolved allowing for the determination of the atomic film composition.

Although RBS is a well established technique for the determination of thickness and sample composition, EPMA is more available and cheaper than RBS. For this reason, the development of a method for thickness determination based on EPMA (and initially calibrated with RBS) is of great interest.

The spectra obtained by α particle excitation were processed with the SIMNRA program [15], to obtain the film thicknesses. Fig. 1 shows, as an illustrative example, the RBS spectra obtained for the samples corresponding to 90 and 5 V induced by 2 MeV α particles. For the first case, it can be seen that in the energy regions corresponding to backscattering events within the titanium oxide layer (around 0.7 MeV for oxygen and 1.3 MeV for titanium) a complex structure appears, which cannot be properly described with a unique stoichiometry. If the studied film were homogeneous in composition, the contribution to the RBS spectrum should be given by a step (starting around 1.45 MeV) due to the interaction with the titanium film atoms, and another step (at around 1.3 MeV) due to the interaction with the substrate atoms. The subtle intensity jump near 1.35 MeV (see Fig. 1) indicates that one region of the film is richer in Ti than the other one; particularly, the layer closer to the substrate. In addition, a careful

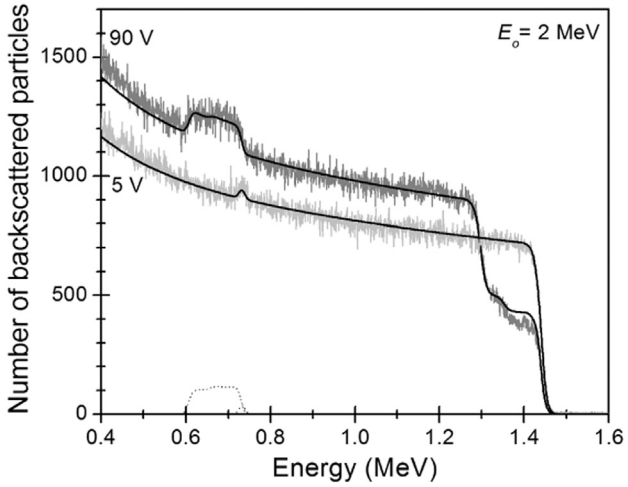

Fig. 1. RBS spectra obtained from samples anodized at 90 V (upper curve) and 5 V (lower curve) induced by 2.00 MeV α-particle excitation. Solid grey line: experimental data; solid black line: fitting; dashed line: contribution of oxygen.

examination of the structure associated with scattering with oxygen atoms (0.60–0.75 MeV) reveals an intensity decrease towards the left side, evidencing a region with less oxygen close to the substrate, as noted also by Serruys et al. [11] and Sul et al. [12].

For this reason, for the samples anodized at 90, 70 and 50 V, a two layer model was assumed as an approximation to the more complex actual profile: TiO_2 at the upper layer and Ti_2O_3 (with higher Ti and lower O concentrations with respect to TiO_2) at the lower one, i.e., the layer in contact with metallic titanium. The lower amount of oxygen found at a greater depth is reasonable and characteristic of any diffusion process. In the case of the thinnest samples, this level of detail is not observable, and a unique TiO_2 layer was assumed.

It can be seen that for 2 MeV spectra, the signal-to-noise ratio worsens for decreasing oxide thicknesses. This worsening introduces greater uncertainties in the thickness determination. To solve this inconvenience, samples anodized at 5, 10 and 15 V were processed following a different strategy: the nuclear reaction $O^{16}(\alpha,\alpha)O^{16}$, occurring at 3.04 MeV [16] was used, taking advantage of the signal intensification produced in the oxygen peak. The RBS spectra produced by α particles with nominal energies of 3.04 and 3.05 MeV for the sample corresponding to 5 V are shown in Fig. 2. As can be observed by comparison with Fig. 1, the signal-to-noise ratio is much higher for the spectra obtained with higher incidence energies, capable to trigger the nuclear reaction mentioned. It can also be seen in Fig. 2 that small variations in the incidence energy modify substantially the signal intensity at energies close to the nuclear reaction characteristic energy. It is therefore important to accurately determine the incident particle energy, which can slightly differ from the nominal value. With this purpose, the beam energy was fitted with SIMNRA in the spectra produced with nominal beam energies of 3.04 and 3.05 MeV, impinging on the 90 V sample. The TiO_2 and Ti_2O_3 thicknesses were taken from the 2 MeV spectrum and kept fixed. The resulting values 3.027 and 3.041 MeV respectively replaced the nominal 3.04 and 3.05 MeV, being introduced as constant parameters in the SIMNRA program to determine the thicknesses from the fitting procedure.

The thicknesses obtained are shown in Table 1. The fitting to the experimental RBS data returns the atomic thicknesses, i.e., number of atoms per area unit; to obtain linear thicknesses the nominal densities of the involved oxides were used: 4.23 g/cm^3 for TiO_2 and 4.49 g/cm^3 for Ti_2O_3. For samples anodized at 5, 10 and 15 V, the thicknesses reported correspond to the average of the values obtained with both beam energies used.

In this case, the error was estimated as the half difference of those two values. For the other samples, the uncertainty was associated with

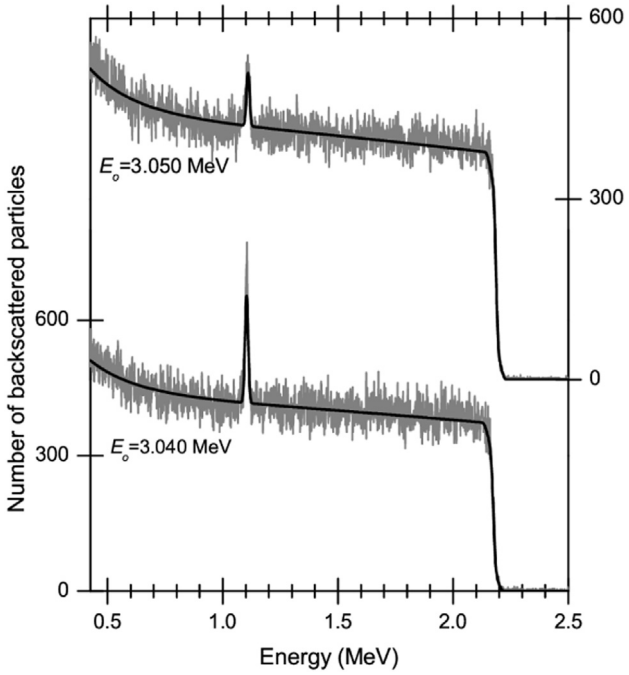

Fig. 2. RBS spectra obtained from the samples anodized at 5 V induced by α-particle excitation with nominal energies of 3.05 MeV (upper curve) and 3.04 MeV (lower curve). Solid grey line: experimental data; solid black line: fitting.

Table 1
Thickness values obtained by RBS for different anodizing voltages. Numbers in parentheses are the estimated uncertainties in the last digits.

Anodizing voltage (V)	Atomic 10^{15} at./cm^2		Linear thickness nm		
	TiO_2	Ti_2O_3	TiO_2	Ti_2O_3	Total
90	990	610	104	60	164 (4)
70	1070	200	112	20	130 (10)
50	660	250	69	25	94 (7)
25	470	–	49	–	49 (7)
20	360	–	38	–	38 (4)
15	200	–	21	–	21 (3)
10	140	–	15	–	15 (3)
5	80	–	8.4	–	8 (2)

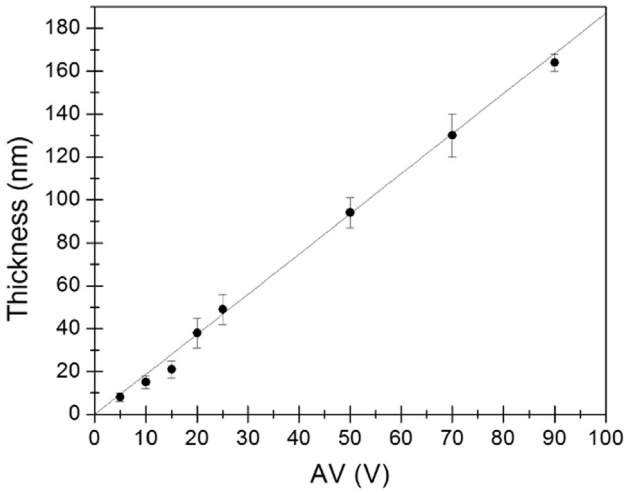

Fig. 3. Thickness values obtained by RBS as a function of anodizing voltage. Dots: experimental data; solid line: linear fit.

the difference between the thicknesses obtained using two independent fitting strategies.

The thickness values obtained by RBS follow a linear behavior with anodizing voltage (see Fig. 3). Bearing this trend in mind, the following relationship was proposed to fit the experimental thickness data (d) as a function of the anodizing voltage (AV):

$$d = a + b\mathrm{AV}{-}0.89 \quad (1)$$

where 0.89 is the onset voltage for oxidation formation expressed in volts, as estimated in [13]. The fitted values were $a = (0 \pm 2)$ nm, and $b = (1.87 \pm 0.04)$ nm/V.

3.2. EPMA

As mentioned at the beginning of this section, in the proposed method, the O-Kα peak intensity is used as an indicator of the anodized oxide layer thickness. The determination of this intensity must be done carefully, since the O-Kα energy is very close to the value corresponding to the titanium L lines (around 70 eV greater). This fact can lead to spectral deconvolution problems, depending on the resolution of the spectrometer used. In order to study the feasibility of the method, a spectrum of the sample anodized at 30 V was registered in the range between 375 and 583 eV, which can be seen in Fig. 4. The most intense peak is the O-Kα line, while at lower energies, two structures corresponding to titanium L lines can be observed: the lines $L_{II}M_{IV}$ ($L\beta_1$) and $L_{III}M_{IV,V}$ ($L\alpha_{1,2}$) appear around 450 eV, and for energies near 390 eV the involved lines correspond to $L_{II}M_I$ ($L\eta$) and $L_{III}M_I$ ($L\ell$) decays [17]. Even when the different lines included in the titanium L spectrum cannot be easily deconvolved, Ti-L and O-Kα peaks are clearly separated with the resolution of the wavelength dispersive spectrometer used. It is worth mentioning that an energy dispersive spectrometer (EDS) has a resolution of around 100 eV at the considered energy, which implies that a reliable deconvolution is impossible with this kind of spectrometer.

Since for the determination of the anodized thickness layer only O-Kα intensity is used, spectra were acquired in an energy range specifically comprising this line for all the samples studied in the present work; this strategy permits to obtain good statistics spectra in reasonable times, with the additional advantage of avoiding sample damage due to long period electron irradiation [13]. The O-Kα peak net intensity was determined by subtracting the background contribution to the peak maximum. The uncertainty in this net intensity was estimated from the statistical dispersion of experimental data in the channels close to the maximum. Net intensities were normalized dividing by the beam current value, which was estimated as the average of the values measured before and after spectrum acquisition. No normalization by

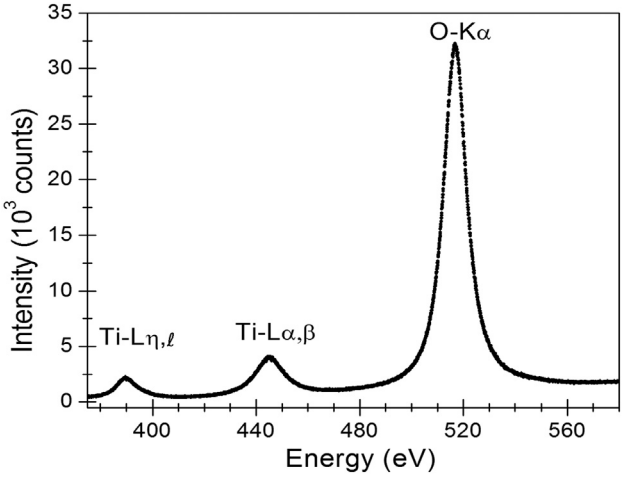

Fig. 4. Spectrum corresponding to the titanium sample anodized at 30 V.

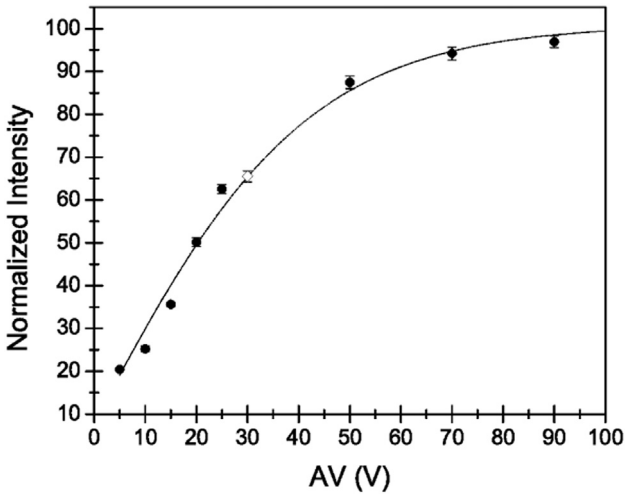

Fig. 5. O-Kα normalized intensity as a function of the anodizing voltage. Solid symbols: experimental data used to carry out the fit; hollow symbol: datum for validation; solid line: fit.

acquisition time was required, since this parameter was kept identical for all the spectra. The error associated with the normalized intensity I was estimated by propagating the errors of net intensity and beam current, which are about 2% and 0.2%, respectively.

Fig. 5 displays the values obtained for the normalized intensities I as a function of the anodizing voltage AV. These experimental data were fitted using the function proposed by Filippin et al. [13]:

$$I = \alpha + \beta \tanh\gamma\mathrm{AV} \quad (2)$$

The parameters obtained from the fit were: $\alpha = 8 \pm 3$, $\beta = 93 \pm 7$ and $\gamma = (0.024 \pm 0.003)\ \mathrm{V}^{-1}$. The final equation to relate thickness with normalized net intensity is obtained from Eqs. (1) and (2):

$$d = b\left[\frac{1}{2\gamma}\ln\left(,\frac{1+\frac{I-\alpha}{\beta}}{1-\frac{I-\alpha}{\beta}}\right){-}0.89\right] + a \quad (3)$$

In Table 2, a comparison between the thickness values measured by RBS and those obtained using Eq. (3) (EPMA-RBS) can be observed. The uncertainty in the thickness calculated by means of this equation was estimated by error propagation, taking into account the fitting errors for the parameters a and b from RBS (Eq. (1)), and for the parameters α, β and γ from EPMA (Eq. (2)). It can be seen that the thicknesses calculated with both methods are indistinguishable considering the associated errors. In addition, the relative difference between values calculated by both methods is lower than 10%, except for two cases. It should be noticed that, according to Eq. (2), a small variation in I is reflected in a large variation in AV for anodizing voltages greater than 70 V (see Fig. 5). This fact is responsible for the large uncertainties

Table 2
Thicknesses for the different anodizing voltages obtained by EPMA and RBS. Numbers in parentheses are the estimated uncertainties in the last digits.

AV (volt)	Thickness (nm)		Relative difference
	RBS	EPMA-RBS	
5	8(2)	9(3)	13%
10	15(3)	13(3)	13%
15	21(3)	22(4)	5%
20	38(4)	36(5)	5%
25	49(7)	51(6)	4%
50	94(7)	97(13)	3%
70	130(10)	130(20)	0%
90	164(4)	150(30)	9%

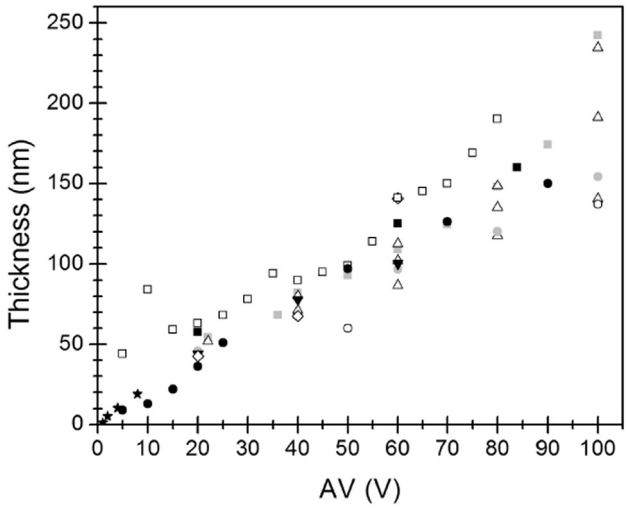

Fig. 6. Thickness as a function of the anodizing voltage. The symbol shape is associated with the different solutions used for anodizing. Black circles: this work; hollow circles: [8] with phosphoric acid; grey circles: [12] with phosphoric acid; black squares: [11] with sulfuric acid; hollow squares: [10] with sulfuric acid; grey squares: [12] with sulfuric acid; up triangles: [12] with acetic acid; down triangles: [12] with calcium hydroxide; rhombi: [12] with sodium hydroxide; stars: [13] with perchloric acid.

Table 3
Detailed analysis of titanium oxide anodic growth on metallic titanium in different experimental conditions. Numbers in parentheses are the estimated uncertainties in the last digit.

Ref.	Anodic solution	AV range (V)	Growth rate (nm/V)	R^2
[12]	H_2SO_4	22–130	2.2 (1)	0.88
[11]	H_2SO_4	20–84	2.0 (2)	0.92
[10]	H_2SO_4	5–80	2.3 (1)	0.75
[12]	H_3PO_4	20–100	1.53 (6)	0.96
[8]	H_3PO_4	50–200	1.52 (8)	0.96
This work	$5\%H_3PO_4/1\%H_3BO_3$	5–90	1.74 (8)	0.988
[12]	CH_3COOH	20–100	1.79 (9)	0.79
[12]	$Ca(OH)_2$	20–60	1.8 (1)	0.90
[12]	Na(OH)	20–60	2.1 (2)	0.91
[13]	$HClO_4$	1–8	2.5 (2)	0.989

associated with thicknesses above 100 nm, as shown in Table 2. It is clear that the method proposed is sensitive to thickness variations as long as this thickness remains clearly below the electron range in the material analyzed. For the beam energy used here, the Kanaya-Okayama range is below 200 nm, and the fitting obtained reliably applies for thicknesses up to approximately half of this range, which is within the scope of the present study. If larger thicknesses are to be determined, higher beam energies must be used, which should be established by estimating the corresponding electron range in the material.

The validity of the relationship obtained between O-Kα intensity and anodizing voltage was tested by comparing the measured intensity to the value calculated by means of Eq. (2) for the spectrum corresponding to a sample anodized at 30 V, not used in the derivation of this equation. As can be seen from Fig. 5, the agreement is very good. The thickness value obtained using Eq. (3) was 57 nm, which is consistent with the trend found between 5 and 90 V (see Table 2).

Thicknesses obtained by means of Eq. (3) are shown in Fig. 6 as a function of AV, along with results obtained by several authors using different methods, voltage ranges and anodizing solutions. It can be observed that, despite the different conditions for the experiments, the growth rates are comparable. A more detailed analysis of the results available in the literature is presented in Table 3. For each data set a linear function was fitted, the slope representing the oxide growth rate. The fitting quality is indicated by the linear regression coefficient R^2. In all the cases the fitting function used is $d = b{\cdot}AV$, except for the cases corresponding to this work and [13], for which Eq. (1) was used. This expression takes into account the onset voltage, which can only influence in the fitting when the analyzed voltages are small.

By comparing the growth rates tabulated, it can be seen that the methods involving H_2SO_4, NaOH and HCl present the greatest values, between 2.0 and 2.5 nm/V. On the other hand, when H_3PO_4 is used, as in the present work, the lowest rates are produced (between 1.52 and 1.74), though it must be noticed that in this work H_3PO_4 is used in solution with H_3BO_3.

4. Conclusion

A method to determine the thickness of titanium oxide layers on metallic titanium has been developed for the range between 5 and 100 nm, of interest in the manufacture of dental and orthopedic implants. Even when the method was developed on the basis of EPMA and RBS measurements, its application through the use of Eq. (3) to other samples of the same kind (TiO_2 layer on Ti substrate) just requires new EPMA measurements, which is much more easily available than performing RBS experiments. This method would permit implant manufacturers to carry out quality control in quantitative analysis of anodizing treatments. This approach can also be extended to larger thicknesses by increasing the incident electron beam energy to an optimum value, according to the thickness range for which it is intended.

The developed method has been validated in a test sample anodized at 30 V, for which the thickness value assessed supports the reliability of the present approach. In addition, the oxide growth rate obtained with the method developed in this work is in agreement with values reported in the literature.

The proposed method can easily be extended to the determination of oxide layer thicknesses formed electrochemically under different experimental conditions; for instance, on the titanium alloy Ti6Al4V, which is widely used as implant material. This alloy forms a layer mainly composed by TiO_2 and Al_2O_3, whose thickness increases with the anodizing voltage. The method developed here could be extended to obtain both oxide layer thicknesses separately, by measuring O-Kα and Al-Kα peak intensities.

Funding

This research received financial funding from the Secretaría de Ciencia y Técnica of the Universidad Nacional de Córdoba (30720130101242CB) and from the Consejo Nacional de Investigaciones Científicas y Técnicas de la República Argentina (CONICET).

Acknowledgements

The authors acknowledge the courtesy of Kinetical SRL for supplying the samples used in this work. They are also grateful to Ing. Carlos Llorente for kindly reviewing the manuscript. Finally, the authors would like to thank the *Centro Atómico Bariloche* and the *Laboratorio de Microscopía Electrónica y Análisis por Rayos X* (LAMARX) of the *Universidad Nacional de Córdoba*, Argentina, where measurements were carried out.

References

[1] X. Liu, P.K. Chu, C. Ding, Surface modification of titanium, titanium alloys, and related materials for biomedical applications, Mat Sci Eng R 47 (2004) 49–121.
[2] M. Navarro, A. Michiardi, O. Castaño, J.A. Planell, Biomaterials in orthopaedics, J R Soc Interface 5 (2008) 1137–1158.
[3] M. Geetha, A.K. Singh, R. Asokamani, A.K. Gogia, Ti based biomaterials, the ultimate choice for orthopaedic implants – a review, Prog Mater Sci 54 (2009) 397–425.

[4] Y.J. Lee, D.Z. Cui, H.R. Jeon, H.J. Chung, Y.J. Park, O.S. Kim, Y.J. Kim, Surface characteristics of thermally treated titanium surfaces, J Periodontal Implant Sci 42 (2012) 81–87.
[5] M. Vallet Regi, L. Munuera, Biomateriales: aquí y ahora, first ed., Dykinson, Madrid, 2000.
[6] E. Gemelli, N.H. Almeida Camargo, Low voltage anodization of titanium in nitric acid solution: a new method to bioactivate titanium, Mater Charact 62 (2011) 938–942.
[7] K. Indira, S. Ningshen, U. Kamachi Mudali, N. Rajendran, Effect of anodization parameters on the structural morphology of titanium in fluoride containing electrolytes, Mater Charact 71 (2012) 58–65.
[8] N.K. Kuromoto, R.A. Simão, G.A. Soares, Titanium oxide films produced on commercially pure titanium by anodic oxidation with different voltages, Mater Charact 58 (2007) 114–121.
[9] E. Krasicka-Cydzik, Anodic layer formation on titanium and its alloys for biomedical applications, in: A.K.M. Nurul Amin (Ed.), Titanium Alloys - Towards Achieving Enhanced Properties for Diversified Applications, InTech, Rijeka, 2012, pp. 175–200.
[10] A. Karambakhsh, A. Afshar, S. Ghahramani, P. Malekinejad, Pure commercial titanium color anodizing and corrosion resistance, J Mater Eng Perform 20 (2011) 1690–1696.
[11] Y. Serruys, T. Sakout, D. Gorse, Anodic oxidation of titanium in 1 M H_2SO_4, studied by Rutherford backscattering, Surf Sci 282 (1993) 279–287.
[12] Y.T. Sul, C.B. Johansson, Y. Jeong, T. Albrektsson, The electrochemical oxide growth behavior on titanium in acid and alkaline electrolytes, Med Eng Phys 23 (2001) 329–346.
[13] F.A. Filippin, O.E. Linarez Pérez, M. López Teijelo, R.D. Bonetto, J. Trincavelli, L.B. Avalle, Thickness determination of electrochemical titanium oxide (Ti/TiO_2) formed in $HClO_4$ solutions, Electrochim Acta 129 (2014) 266–275.
[14] F. Salvat, J.M. Fernández-Varea, J. Sempau, PENELOPE—A Code System for Monte Carlo Simulation of Electron and Photon Transport, OECD/NEA Data Bank, Issy-les-Moulineaux, France, France, 2003.
[15] M. Mayer, SIMNRA User's Guide, Report IPP 9/113, Max-Planck-Institut f¨ur Plasmaphysik, Garching, Germany. http://home.mpcdf.mpg.de/~mam/, (1997).
[16] J.W. Mayer, E. Rimini, Ion Beam Handbook for Material Analysis, first ed., Academic Press, New York, 1977.
[17] J.A. Bearden, X-ray wavelengths, Rev Mod Phys 39 (1967) 78–124.